

# NONLINEAR FINITE ELEMENT ANALYSIS OF INSULATED FRP STRENGTHENED REINFORCED CONCRETE COLUMNS SUBJECTED TO FIRE

*Osama El-Mahdy, Gehan Hamdy and Mohamed Hisham*

*Department of Civil Engineering, Faculty of Engineering at Shoubra, Benha University, Shoubra, Cairo, Egypt; [osama.alhenawy@feng.bu.edu.eg](mailto:osama.alhenawy@feng.bu.edu.eg); [os8294@hotmail.com](mailto:os8294@hotmail.com)*

## ABSTRACT

In recent decades, Fiber Reinforced Polymers (FRP) have shown tremendous potential for retrofitting or repairing existing deficient or damaged concrete structural elements due to their superior properties such as high strength, corrosion resistance and ease of application. However, concern arises about the vulnerability of FRP material to combustion under fire condition, since they are usually applied to the exterior surface of structural members. Damage of the FRP strengthening layer due to high temperature is likely to decrease the load carrying capacity of the columns and threaten the safety of the structure. This paper presents numerical investigation of the behaviour of reinforced concrete (RC) columns strengthened with FRP sheets and insulated by a thermal resisting coating under service load and fire conditions. The finite element numerical modelling and nonlinear analysis are made using the nonlinear finite element analysis software ANSYS 12.1 [1]. The numerical model is verified for several FRP confined and insulated RC columns that have been experimentally tested under service load and standard fire tests in the published literature. The obtained numerical results are in good agreement with the experimental ones regarding the temperature distribution and axial deformation response. Consequently, the presented modelling gives an economic tool to investigate the behaviour of loaded FRP strengthened RC columns under high temperatures occurring in case of fire, if the modelling is verified against experimental works. Furthermore, the model can be used to design thermal protection layers for FRP strengthened RC columns to fulfill fire resistance requirements specified in building codes and standards.

## KEYWORDS

Numerical modelling, RC columns, FRP, Elevated temperature, Thermal insulation

## INTRODUCTION

The increasing use of FRP in strengthening applications is due to their high strength, durability and excellent corrosion resistance, in addition to small added thickness and ease of application. However, their inferior performance under fire condition presents a threat to the strengthened member since they are usually applied on the outer surface of the structural elements and the strengthening may be totally lost in case of fire [2]. One of the most popular applications of FRP is strengthening of reinforced concrete (RC) columns. This can be done by two different ways, first by applying FRP sheets to the longitudinal direction of the column in order to provide additional flexural strength, or by applying FRP sheets in circumferential direction in order to provide confining reinforcement which increases both axial load capacity and ductility of the

column. Steel spirals or hoops have been widely used in confinement of RC columns, yet they are heavy, difficult to install and corrosive. FRPs provide a competitive solution, being non-corrosive, lightweight and easy to install. Youssef et al. [3] developed a semi-empirical model for FRP confinement for circular and rectangular RC column sections based on large scale experimental program to predict the confined strength ( $f'_{cu}$ ) and confined axial strain ( $\epsilon_{cu}$ ).

Experimental studies were carried out to investigate the performance of FRP strengthened RC columns under service load and fire condition by several researchers [4-6]. In order to provide protection of FRP from fire exposure, a coating layer material of good thermal resisting properties, typically gypsum products, may be placed around the columns. In fire test programs conducted by these researchers, RC columns strengthened by multiple layers of carbon fiber reinforced polymers (CFRP) and protected with coatings of different types and thickness were exposed to standard fire load of ASTM E119 [7] while being subjected to service loads. Experimental and numerical results for both thermal and structural aspects were presented. Using insulation layer with proper thickness was capable of increasing the fire resistance time to over five hours of fire exposure [4].

However, few studies in the published literature addressed numerical modelling to predict the structural or thermal behaviour of FRP-confined RC members subjected to fire with multiple types of protection systems [4,8]. Hence, more investigation work is required to model efficiently the behaviour of FRP-strengthened RC columns under elevated temperatures in order to enable designers to accurately predict the fire resistance time and residual strength after fire exposure and provide a reliable tool for design of thermal insulation layers for these columns.

## OBJECTIVE

The present paper aims to study numerically the behaviour of RC columns confined by FRP and thermally protected with insulation material under service load and standard fire test loading. To achieve this goal, numerical modelling by finite elements is made that represents the column geometry, boundary conditions, load variation and considers the variation in thermal and mechanical properties of the different constituent materials with elevated temperature. Numerical modelling and nonlinear analysis are made using the software ANSYS v.12.1.0 [1]. A numerical study is conducted on FRP confined and insulated columns that have been previously tested experimentally under standard fire test. The numerical thermal and structural results are presented and compared to published experimental and numerical results so as to verify the adequacy of the adopted numerical procedure. Finally, the conclusions of the study are given.

## VARIATION OF MATERIALS PROPERTIES WITH ELEVATED TEMPERATURE

### Density

The density ( $\rho$ ) of concrete varies with raising the temperature as given by Eurocode 2 [9], and is shown in Figure 1. The steel reinforcement density is stated by Eurocode 3 [10] to remain constant under elevated temperature. The FRP density stays constant up to approximately 550°C then it has slight decrease. After that, it stays constant until 1000°C (Griffis et al. 1984) [11] as shown in Figure 2. The relations shown in the figures are plotted as normalized density related to density at room temperature.

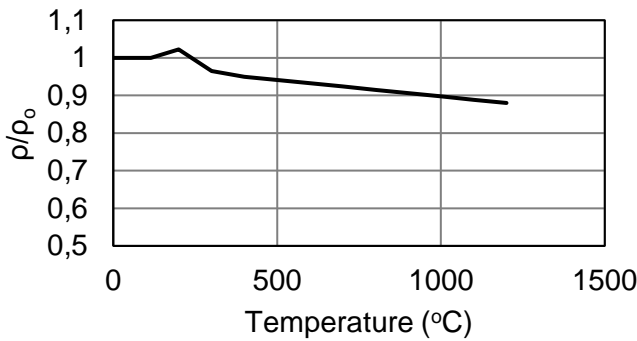


Fig. 1 - Variation of density of concrete with temperature [9]

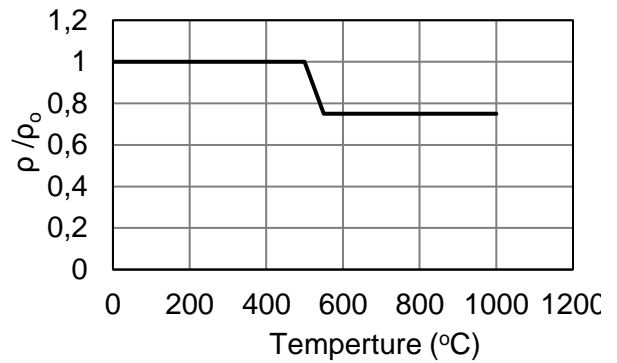


Fig. 2 - Variation of density of FRP with temperature [11]

### Thermal Conductivity

The variation of thermal conductivity of concrete with elevated temperature is given by Eurocode 2 [9] and shown in Figure 3. Figure 4 illustrates the variation in thermal conductivity for steel reinforcement with elevated temperatures as given by Eurocode3 [10]. Based on the data provided by Griffis et al. [11], FRP materials have low thermal conductivity and thermal conductivity of FRP seems to decrease with elevated temperatures as shown in Figure 5.

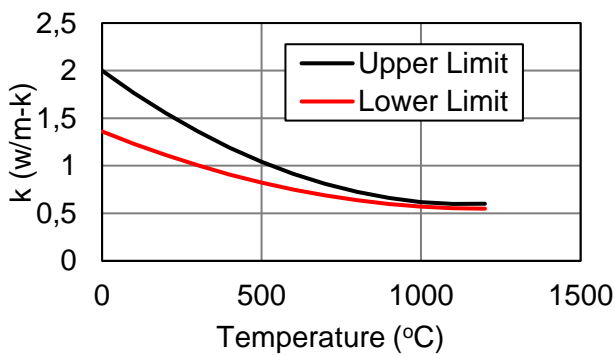


Fig. 3 - Variation of thermal conductivity of concrete with temperature [9]

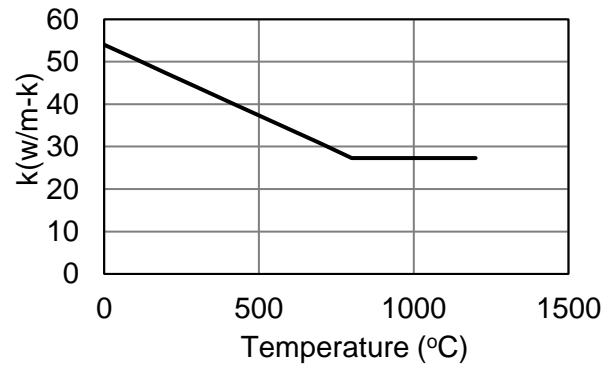


Fig. 4 - Variation of thermal conductivity of steel with temperature [10]

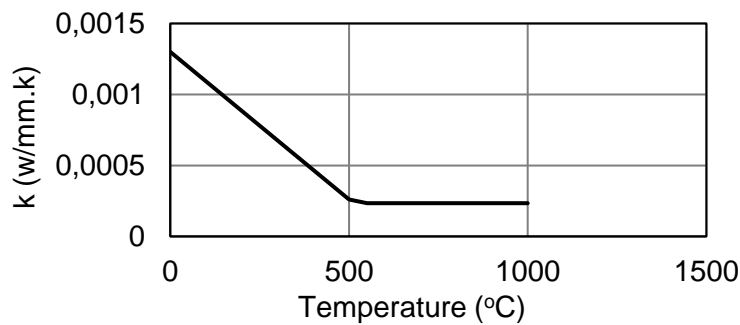


Fig. 5 - Variation of thermal conductivity of typical FRP with elevated temperatures [11]

### Specific Heat

The variation of specific heat of concrete with elevated temperature is given by Eurocode 2 [9] and shown in Figure 6. Based on the experimental data provided in Eurocode 3 [10], the specific heat of steel with elevated temperature is shown in Figure 7. The complex chemical reactions under high temperature with the composite are the reason behind the irregularity behaviour of the specific heat of FRP material (Griffis et al.,) [11] as shown in Figure 8.

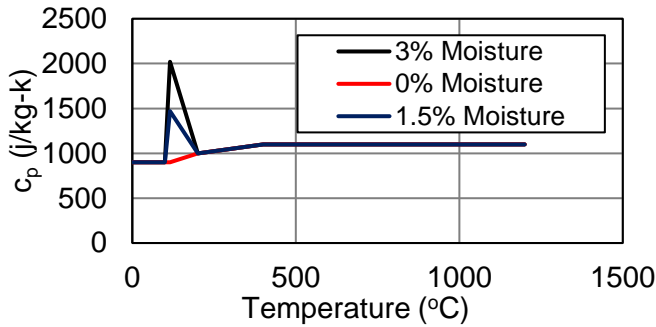


Fig. 6 - Variation of concrete specific heat at elevated temperatures [9]

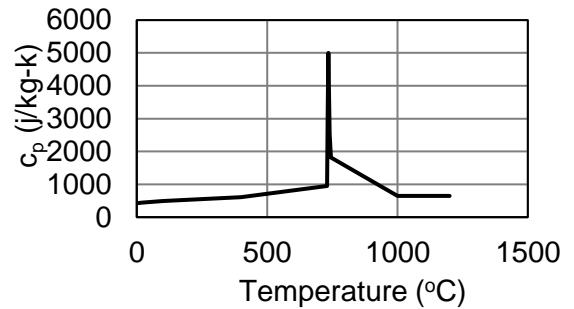


Fig. 7 - Variation of specific heat of steel with elevated temperatures [10]

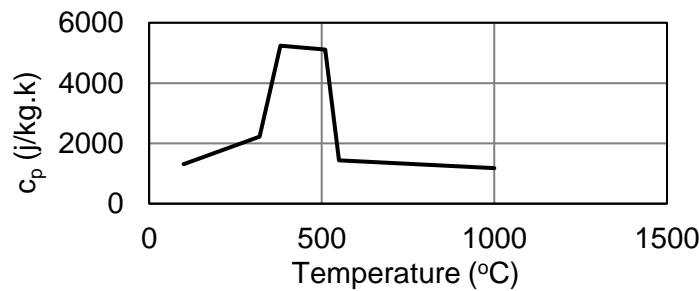


Fig. 8 - Variation of specific heat of typical FRP with elevated temperatures [11]

### Strength and Modulus of Elasticity

The elastic modulus mainly depends on the compressive strength of concrete as given by Eurocode 2 [9] in Equation (1).

$$E_c = 5000 \sqrt{f'_c} \tag{1}$$

As shown in Figure 9, concrete with carbonate aggregate experiences slower degradation rate of its compressive strength at elevated temperatures compared to siliceous aggregate concrete. Variation of tensile strength of concrete with temperature is given by Eurocode 2 [9] as shown in Figure 10.

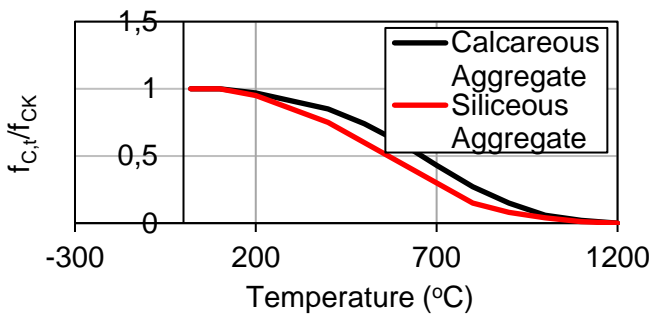


Fig. 9 - Variation of compressive strength of concrete with temperature [9]

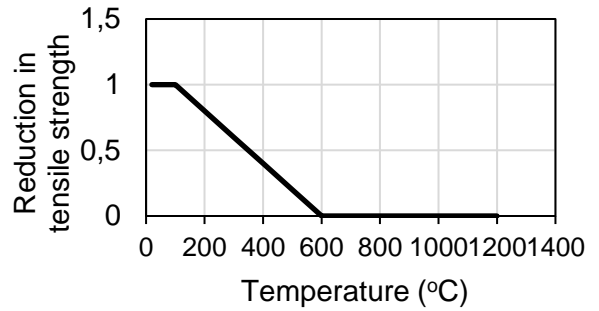


Fig. 10 - Reduction of concrete tensile strength with elevated temperatures [9]

As shown in Figure 11, steel loses more than 50% of its original strength at about 600°C [10]. Likewise, it is clear from Figure 12 that, the modulus of elasticity of the reinforcement steel decreases with elevated temperature.

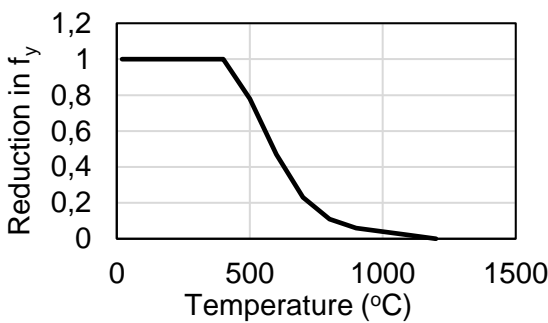


Fig. 11 - Reduction of yield strength of steel with elevated temperatures [10]

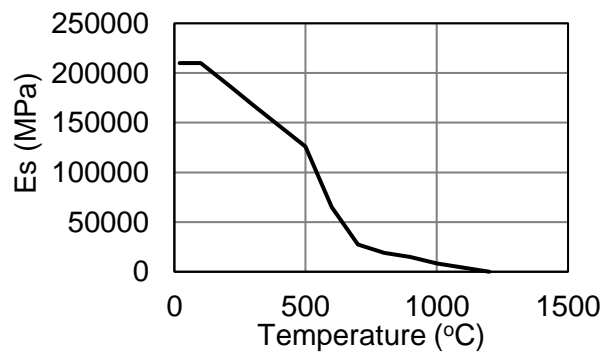


Fig. 12 - Reduction in modulus of elasticity of steel with elevated temperatures [10]

Figure 13 shows the reduction in strength of CFRP and GFRP with elevated temperature. Likewise, stiffness of FRP materials also has similar rapid degradation with elevated temperature as shown in Figure 14.

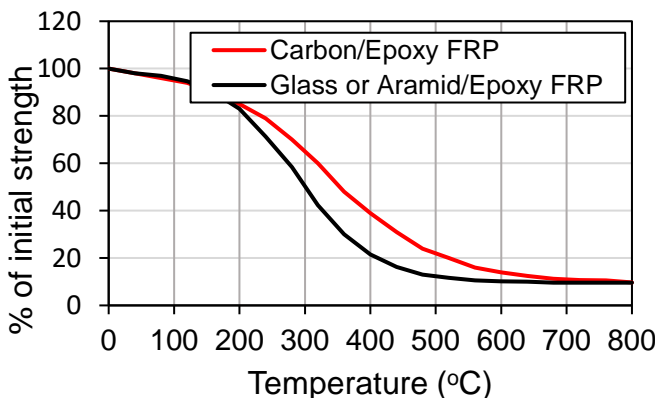


Fig. 13 - Reduction in strength for various FRP materials with elevated temperatures [4]

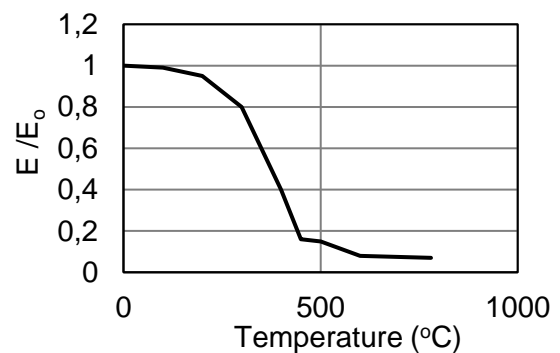


Fig. 14 - Reduction of stiffness of CFRP with elevated temperatures [12]

### Thermal Expansion

The variation of thermal expansion is shown in Figure 15 as given by Eurocode 2 [9] for concrete containing two aggregate types. Thermal expansion of steel reinforcement increases with the increase in temperature as given Eurocode 3 [10] and shown in Figure 16.

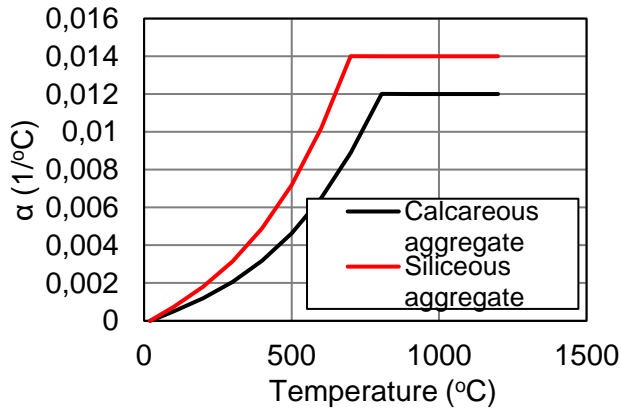


Fig. 15 - Variation of thermal expansion of concrete with temperature [9]

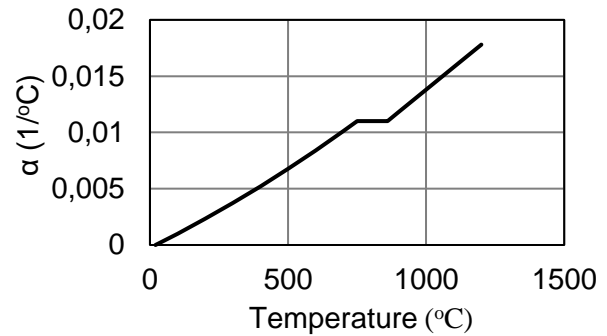


Fig. 16 - Coefficient of thermal expansion of steel with elevated temperatures [10]

### Transient Creep

Transient creep is an additional non-recoverable strain that develops only during first time heating of concrete member under compression load as illustrated in Figure 17. Transient creep is load induced thermal strain that happens due to the shrinking of cement matrix and loss of water during heating. In this case total strain has three components, mechanical strain, expansion strain and transient creep strain [13]. It should be noticed that the thermal expansion strain has different direction from the other strains.

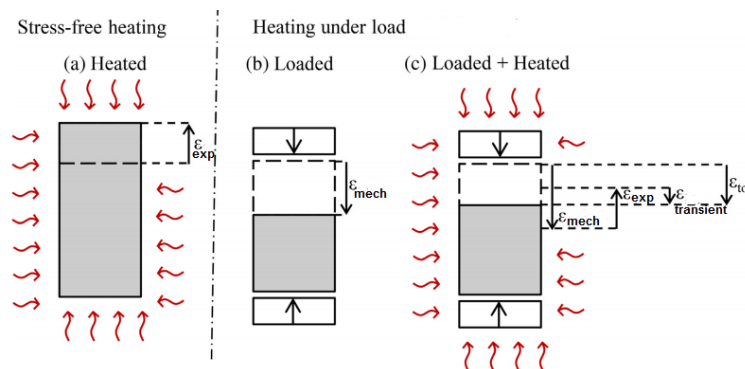


Fig. 17 - Different types of strains under heat, load or both effects [13]

Anderberg and Thelandersson [14] proposed a model for predicting transient creep which is linearly proportional to the applied stress and thermal expansion strain of aggregate according to Equation (2).

$$\epsilon_{tr} = K \left( \frac{\sigma}{\sigma_u} \right) \epsilon_{exp} \quad (2)$$

where  $K$  is the factor that depends on aggregate type and is equal to 1.8 for siliceous aggregate and 2.35 for carbonate aggregate,  $\sigma$  is the applied stress,  $\sigma_u$  is the compressive strength and  $\epsilon_{exp}$  is the thermal expansion of aggregate.

### Thermal Properties of Insulation Materials

Three types of thermal insulation are used in this numerical study namely; Vermiculite-Gypsum (VG), MBrace and Sikacrete. VG Insulation product is the most favourable material in fire protection manufactured by Tyfo®. This insulation consists of two materials; gypsum and vermiculite. Insulation materials properties variations under elevated temperature are presented in Figures (18-20) [15,16].

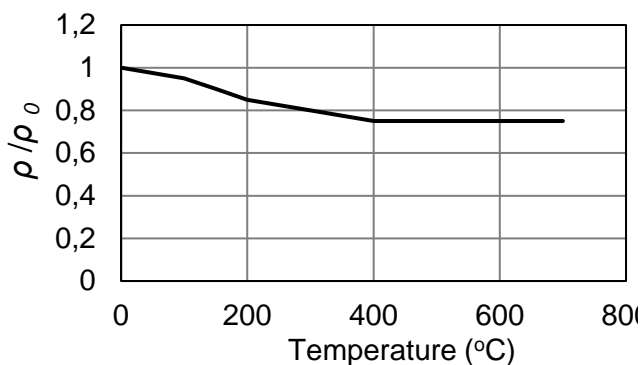


Fig. 18 - Variation of density of VG insulation with temperature [15,16]

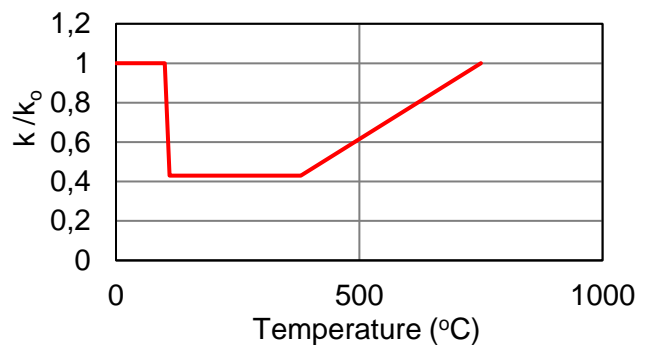


Fig. 19 - Variation of thermal conductivity of VG insulation with temperature [15,16]

The MBrace is a spray applied cementitious mortar based containing various insulating fillers which prevents degradation of concrete mechanical properties above 300°C. As reported by Chowdhury et al., [5] density and thermal conductivity of MBrace at room temperature were known from manufacturer only and the variation of MBrace thermal properties with elevated temperature was not available, therefore assumptions of the thermal properties are made in this study. The thermal conductivity is assumed to remain constant during duration of fire exposure. Furthermore, since MBrace insulation is cementitious mortar based material, the variation of the specific heat with elevated temperature was assumed to be similar to that of the specific heat of carbonate aggregate concrete as suggested by Lie et al., [17] and shown in Figure 21.

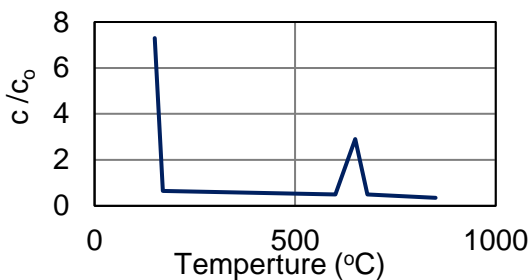


Fig. 20 - Variation of specific heat of VG insulation with temperature [15,16]

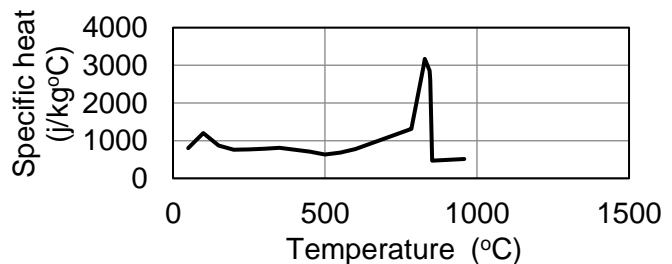


Fig. 21 - Specific heat of carbonate aggregate concrete [17]

The Sikacrete®-213F is a spray applied mortar based protection system with vermiculite and acts as the insulating filler, which gives strong thermal insulation properties. As reported by Masoud et al., [18] the density of Sikacrete is equal to 700 Kg/m<sup>3</sup> and the variations in thermal conductivity and specific heat are given by Eqs. (3) and (4), respectively.

$$Kc(T) = 0.46 \left( \frac{T}{1000} \right)^2 - 0.21 \left( \frac{T}{1000} \right) + 0.32 \quad \text{in} \left( \frac{W}{m.K} \right) \quad (3)$$

$$Cc(T) = 14.96 \left( \frac{T}{100} \right)^2 - 116.4 \left( \frac{T}{100} \right) + 1611 \quad \text{in} \left( \frac{J}{Kg.K} \right) \quad (4)$$

## MODELLING AND NONLINEAR SOLUTION METHODOLOGY

The general approach for performing the thermal and structural modelling and nonlinear analysis are summarized in Figure 22, the main steps include:

1. Building 3-D nonlinear numerical model of the RC column. This process includes member geometry, appropriate definitions for the materials of concrete, reinforcement steel, FRP and boundary conditions. Two separates finite element models were created, one for thermal analysis and the other for structural analysis.
2. Applying the thermal loads in the form of transient temperatures versus time to the outer surface of column by utilizing regime function method in ANSYS. The thermal load is applied according the ASTM E119 [7].
3. After comparing and verification of the predicted with measured temperatures in the cross section of the column, the temperature data is used in the load step information of the structural model.
4. Applying service load and the predicted thermal loads into the structural model through two cumulative load steps. In case of earlier non-convergence problem has occurred, kill and birth technique is used to exclude the crushed elements from matrix and continue the solution.
5. If the column did not fail after 5 hours of fire exposure, the service load will be increased gradually through regime function method in ANSYS to induce failure.
6. Evaluate the vertical displacement of the column during the fire exposure time to the fire and comparing it with experimental measured ones.

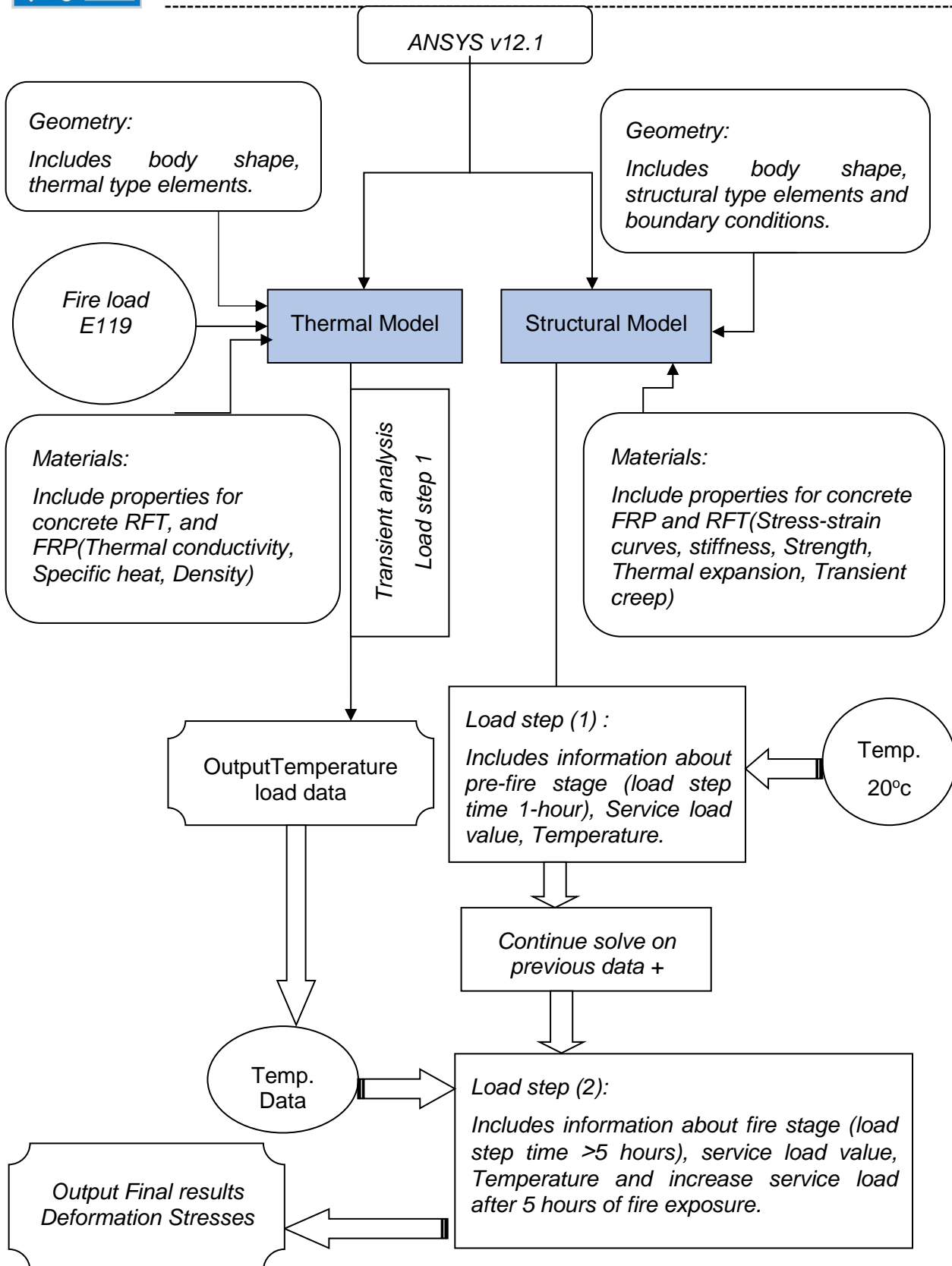


Figure 22: Schematic modeling methodology for RC columns strengthened with FRP

## NUMERICAL VERIFICATION STUDY

A numerical study was conducted for verification of the proposed model for FRP strengthened RC columns subjected to elevated temperatures due to fire. Four studied experimental cases by other researchers are chosen for the verification. Table (1) gives a summary of these cases. The first two columns were tested by Bisby [4], the third column was tested by Chowdhury et al., [5], while the last column was tested by Cree et al., [6].

*Tab. 1 - Summary of the case studies data*

Case study	Diameter (mm)	Length (mm)	Longitudinal steel bars	Transverse steel bars	f <sub>c</sub> (MPa)	FRP wrap	Insulation (mm)	Service load (KN)
1	400	3810	8T20	11.3 mm spiral at 50 mm pitch	40	1-layer CFRP	32-VG	2515
2	400	3810	8T20	11.3 mm spiral at 50 mm pitch	39	1-layer CFRP	57-VG	2515
3	400	3810	8T20	11.3 mm spiral at 50 mm pitch	32.9	2-layers CFRP	53-MBrace	2635
4	400	3810	8T20	10 mm spiral at 50 mm pitch	38.5	2-layers CFRP	44-Sikacrete	3054

## Element Types for Representation

The element types used to represent the different materials for all columns are given in Table 2. Each type of analysis required specific types of elements in order to get a realistic solution.

*Tab. 2 - Element types used for thermal and structural analyses*

Material	Thermal analysis	Structural analysis
Concrete	SOLID70	SOLID65
Steel bars	LINK33	LINK8
CFRP layer	SHELL57	SHELL41
Insulation	SOLID70	SOLID45

## Description and Geometry

All columns were experimentally tested in the National Research Council in Canada (NRC) using special furnace which is capable of applying elevated temperature according to standard fire test ASTM E119 [7] and service load via hydraulic jack. All columns have circular section with concrete cover of 40 mm and wrapped with CFRP sheets along their full length. The sections of the columns are symmetric about x and z axes therefore, only quarter of the section was modelled in ANSYS, the finite element meshing is shown in Figure 23.

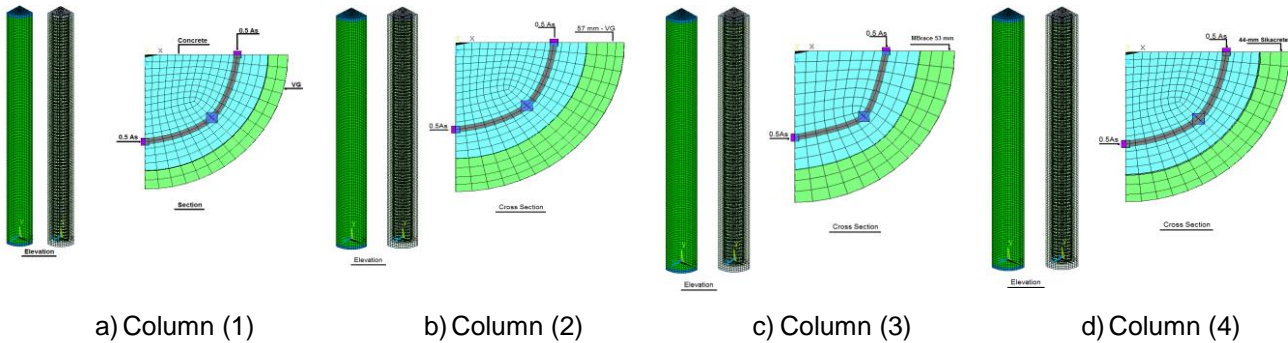


Fig. 23 - Finite element 3-D model of columns in ANSYS

### Materials Properties at Room Temperature

The average concrete compressive strength was taken as given in Table (1), yield strength for longitudinal and transverse reinforcements was 400 MPa for first two columns while they equal to 456 and 396 MPa, respectively for the last two columns. All RC columns were fabricated by carbonate aggregate except for column (3) which was fabricated with siliceous aggregate. The CFRP tensile strength is equal to 1351 MPa for columns (1,2), 3800 MPa for column (3) and 849 MPa for column (4). The stress-strain curve for confined RC section by FRP Youssef et al., [3] was used in this model for different temperature as shown in Figure (24). The rest properties of constituent materials are taken from references [4, 5, 6 and 20].

For RC columns confined with both FRP jacket and steel spiral, the stress-strain curve is influenced by the ratio of lateral confinement pressure of FRP ( $f_{1f}$ ) to the ratio of lateral confinement pressure of steel spiral ( $f_{1s}$ ). Approximately, the lateral confinement pressure of confined concrete by both FRP and steel spiral is equal to the sum of lateral confinement pressure of FRP and lateral confinement pressure of steel spiral as proposed by (Lee et al.2004) [19].

The confinement pressure of FRP depends on the strength of FRP sheet which decreases with elevated temperature as discussed earlier. Bisby [4] observed that 90% of the mass of the S-Epoxy was lost in the temperature range of 390°C to 510°C and auto-ignition of the S-Epoxy occurred at approximately 450°C. Therefore, in order to represent this observation in the numerical model, the lateral pressure of FRP was assumed approximately equal to zero after 400°C, whereby the remaining confining pressure mainly comes from steel spirals confinement for higher temperatures.

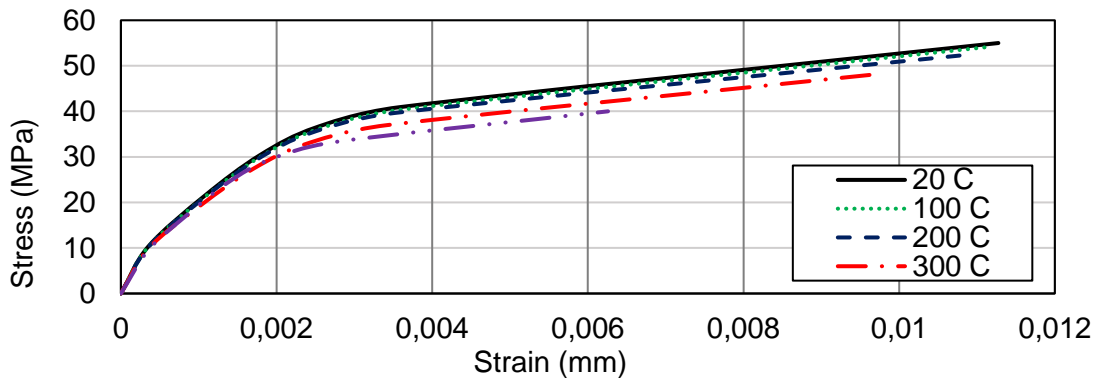


Fig. 24 - Variation of stress-strain relations for confined concrete with temperature

### THERMAL NUMERICAL RESULTS

Figure 25 shows the temperature distribution through the section of column (1) after one, two, three and five hours of exposure. Furthermore, the obtained thermal results using the present model as well as the experimental results obtained by other researchers for the four columns are shown in Figures. 26-29.

For column (1) in Figure 26, the temperature between FRP and concrete changes from room temperature up to 425°C experimentally and 440°C numerically with 3.5% variance after five hours, however, the overall average variance is approximately 24%. As for RFT, temperature increases up to 200°C experimentally and 237°C numerically with 19% variance after five hours, however, the overall average variance is 14%. As for concrete, temperature increases up to 165°C experimentally and 124°C numerically with 25% variance after five hours, however, the overall average variance is 17%. For column (2) in Figure 27, the temperature between FRP and concrete changes from room temperature up to 180°C experimentally and 258°C numerically with 43% variance after five hours, however, the overall average variance exceeds 50%. This happened because the temperature of FRP from first hour to fourth hour remained unchanged below 100°C regardless the continuous heat transfer. As for RFT, temperature increases up to 104°C experimentally and 130°C numerically with 25% variance after five hours, however, the overall average variance is 20%. As for concrete, temperature increases up to 92°C experimentally and 95°C numerically with 3.3% variance after five hours, however, the overall variance is 12%. For column (3) in Figure 28, the temperature between FRP and concrete changes from room temperature up to 480°C experimentally and 460°C numerically with 4% variance after five hours, however, the overall average variance is 12%. As for RFT, temperature increases up to 280°C experimentally and 276°C numerically with 2% variance after five hours, however, the overall average variance is approximately 15%. As for concrete, temperature increases up to 200°C experimentally and 185°C numerically with 8% variance after five hours, however, the overall variance is 27%. For column (4) in Figure 29, the temperature between FRP and concrete changes from room temperature up to 420°C experimentally and 440°C numerically with 5% variance after four hours, however, the overall average variance is 9%. As for concrete, temperature increases up to 180°C experimentally and 220°C numerically with 23% variance after four hours, however, the overall variance is 17%. In general, it can be concluded that the numerically predicted results are in good agreement with experimental ones. The main reason for the variances in prediction temperature mentioned above is generally due to information lack of actual initial values or actual variation with temperature for thermal conductivity, specific heat and density of the used materials in the conducted experiments. These data are not always available from researchers or manufacturers, therefore, standard curves for thermal properties which are discussed in literature have been used in this analysis.

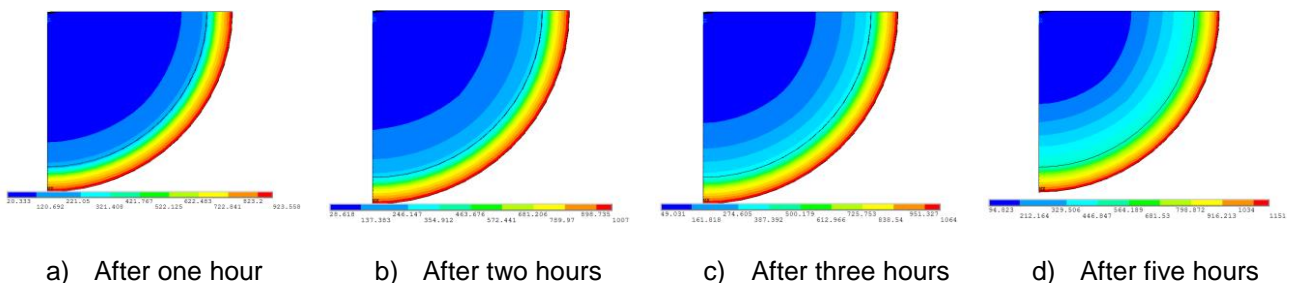


Fig. 25 - Column (1): Numerically predicted temperature distribution in the column cross-section

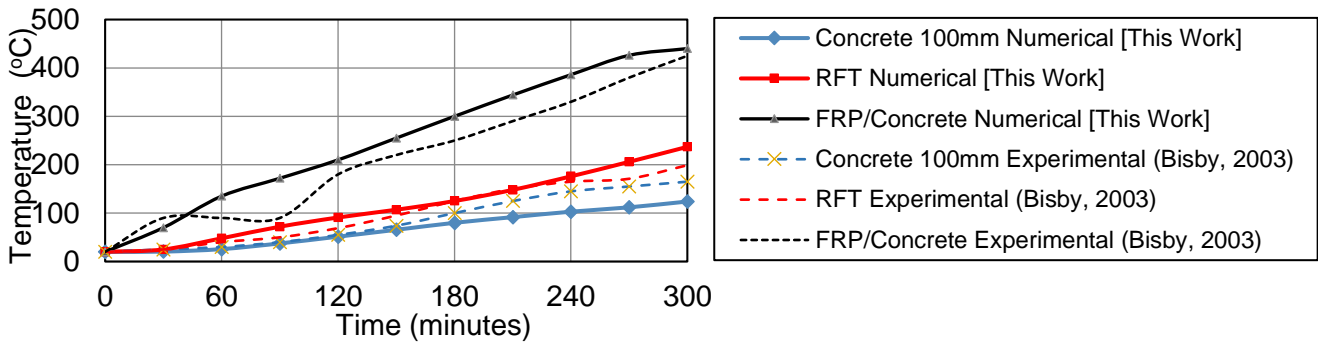


Fig. 26 - Column (1): Numerical thermal results compared to published results

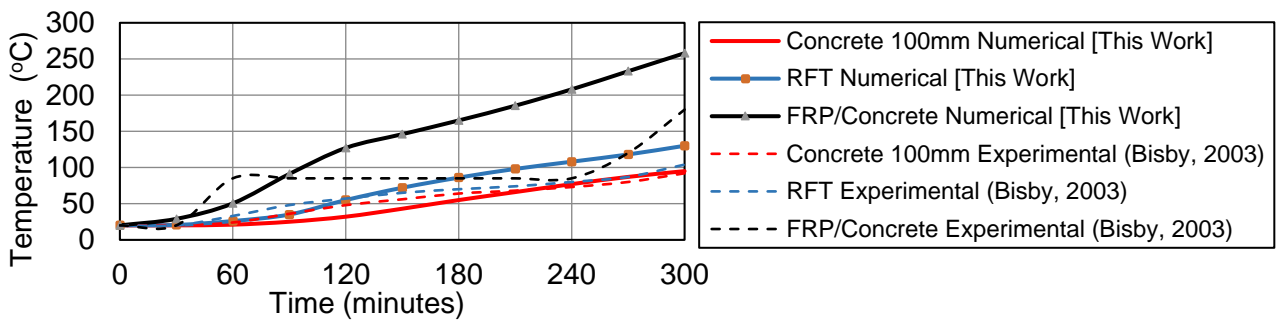


Fig. 27 - Column (2): Numerical thermal results compared to published results

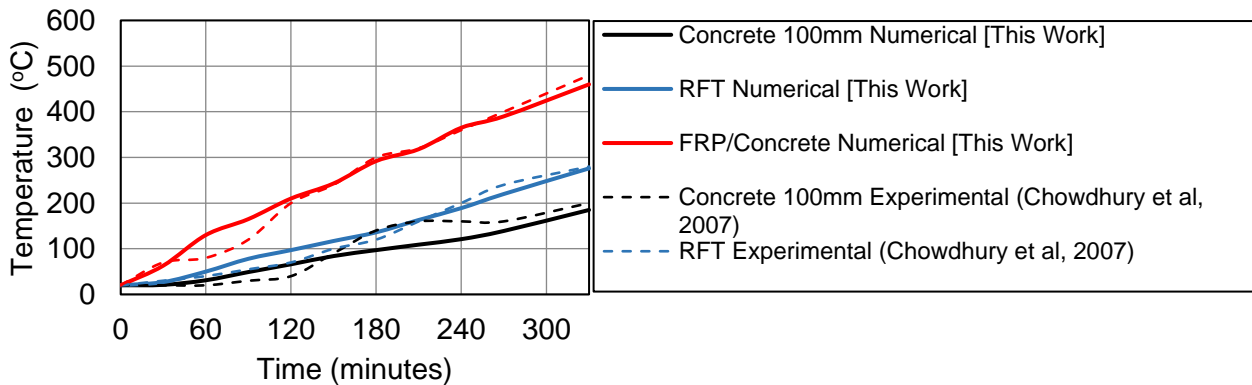


Fig. 28 - Column (3): Numerical thermal results compared to published results

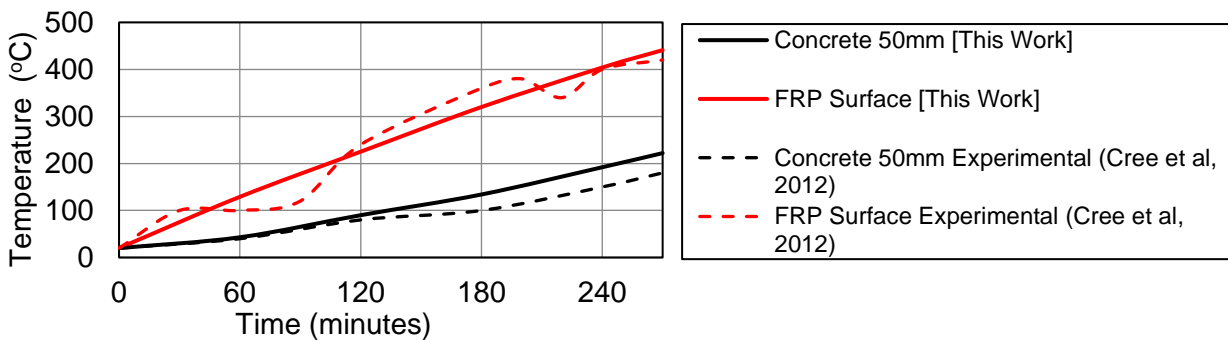


Fig. 29 - Column (4): Numerical thermal results compared to published results

### STRUCTURAL NUMERICAL RESULTS

The obtained structural results for the numerically predicted axial deformation under applied service load and fire exposure for specific time are plotted in Figures 30-33 for the four studied columns, and results are compared to the axial deformation measured in published experimental works. From these figures, it can be observed that the numerically predicted results are in good agreement with experimental ones. For column (1) shown in Figure 30, the main deformation is small elongation till first two hours, then elongation strain decreases due to increase of transient creep strain with elevated temperature which may acts against elongation strain until crushing of column. Elongation strain has more influence than transient creep strain in column (2) shown in Figure 31 due to lower exposed of temperature comparing with column (1). As for columns (3,4) shown in Figures 32, 33, columns experienced elongation strain in first two hours then transient creep strain starts to influence the overall deformations.

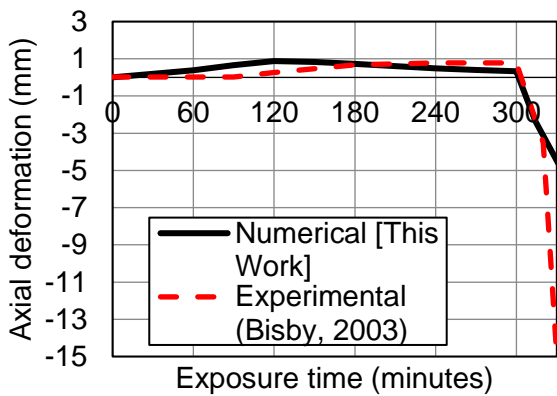


Fig. 30 - Column (1): Axial deformation of the column during fire exposure

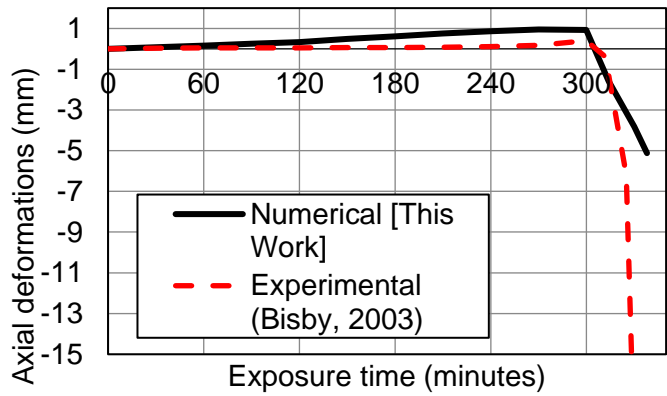


Fig. 31 - Column (2): Axial deformation of the column during fire exposure

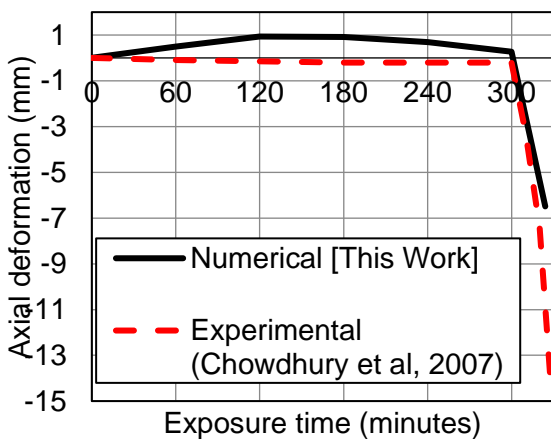


Fig. 32 - Column (3): Axial deformation of the column during fire exposure

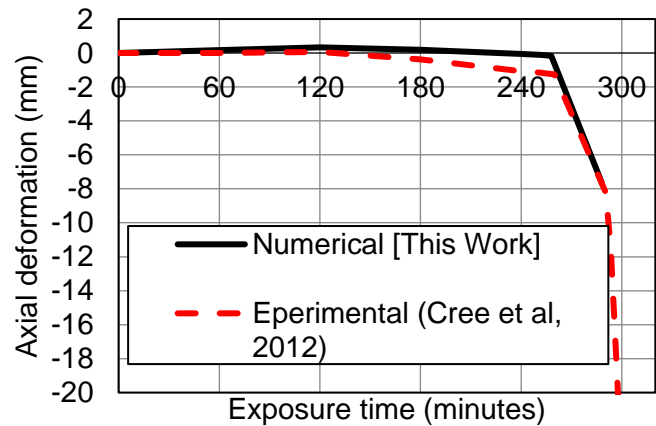


Fig. 33 - Column (4): Axial deformation of the column during fire exposure

Table 3 summarizes the numerically predicted and experimental results and provides the ultimate capacity of the columns at normal temperature 20°C.

*Tab. 3 - Summary of experimental and numerically predicted results*

Case study	Fire resistance (min)		Failure load (KN)		Variance in failure load	Predicted capacity at ambient temperature (KN)
	Experimental	Numerical	Experimental	Numerical		
1	>300	>300	4473	5018	1.12	5800
2	>300	>300	4680	5393	1.15	5800
3	>300	>300	4583	4682	1.02	5600
4	>240	>240	4980	5647	1.13	6600

## CONCLUSIONS

The paper presents numerical modelling procedure by finite elements that simulate the performance of RC column strengthened with CFRP sheets and thermally insulated when exposed to standard fire test under service loads. Numerical modelling and nonlinear analysis are performed using the general purpose software ANSYS 12.1. The proposed procedure is verified by comparing the numerical results with experimental results available in the published literature. Based on the obtained numerical results, the following conclusions can be drawn.

1. The numerically predicted results of the proposed model are in good agreement with published experimental results for both thermal and structural aspects. The accuracy of thermal prediction for FRP, RFT and concrete are 78%, 84% and 82%, respectively. Also, for structural failure load prediction, the accuracy is 89%.
2. The proposed model can accurately predict thermal and structural response for different configurations regarding constituent material properties or insulation type and thickness.
3. The proposed model provides a reasonable accurate axial deformation response due to consideration of transient creep strain in the analysis.
4. The axial deformation response for column under fire tend to expand in early stage of fire exposure followed by contraction due to degradation in stiffness and presence of transient creep strain which acts against expansion strain of burned RC column.
5. The proposed model provides an economic tool for check and design of fire insulation layers for FRP strengthened RC columns. It should be noticed that, the modelling needs to be verified against experimental works.

## REFERENCES

1. ANSYS–Release Version 12.1.0, “A Finite Element Computer Software and User Manual for Nonlinear Structural Analysis”, ANSYS Inc. Canonsburg, PA., (2009).
2. Chowdhury,E.U., “Behavior of Fiber Reinforced Polymer Confined Reinforced Concrete Columns Under Fire Condition.”, PhD thesis, Dept. of Civil Engineering Queen’s Univ., Kingston, Ont., Canada, (2009).
3. Yousef, M. N., Feng, M. Q.and Mosallam, A. S., “Stress-Strain Model for Concrete Confined by FRP Composites”, Composites Part B, V. 38, pp. 614-628, (2007).
4. Bisby, L. A., “Fire Behavior of FRP Reinforced or Confined Concrete.”, PhD thesis, Dept. of Civil Engineering Queen’s Univ., Kingston, Ont., Canada, (2003).
5. Chowdhury,E.U., Bisby, L.A. and Green, M.F., "Investigation of Insulated FRP-Wrapped Reinforced Concrete Columns in Fire", Fire Safety Journal, 42 (2007),pp. 452–460.

6. Cree, C., Chowdhury, E.U., Bisby, L.A., Green, M.F., and Benichou, N., "Performance in Fire of FRP-Strengthened and Insulated Reinforced Concrete Columns", *Fire Safety Journal*, 54 (2012), pp. 86–95.
7. ASTM, "Standard Test Methods for Fire Tests of Building Construction and Materials", ASTM Standard E119, American Society for Testing of Materials, West Conshohocken, PA, (2002).
8. Bisby, L.A., Green, M.F. and Kodur, V.K.R., "Modeling the Behavior of Fiber Reinforced Polymer-Confined Concrete Columns Exposed to Fire", 10.1061/(ASCE)1090-0268(2005)9:1(15).
9. Eurocode2, "Design of Concrete Structures, ENV EC2 Part 1.2", Eurocode, (2004).
10. Eurocode 3, "Design of Steel Structures, ENV EC3 Part 1.2.", Eurocode, (2005).
11. Griffis, C., Masmura, R. and Chang, C., "Thermal Response of Graphite Epoxy Composite Subjected to Rapid Heating", *Environmental Effects on Composite Materials*, Vol. 2, pp. 245- 260, (1984).
12. Williams, B, Kodur, V, Green, M. and Bisby, L., "Fire Endurance of Fiber-Reinforced Polymer Strengthened Concrete T-Beams," *J ACI Structural*, vol. 105, No. 1, pp. 60-67, (2008).
13. Torelli, G., Mandal, P., Gillie, M. and Tran, V.X., "Concrete Strains under Transient Thermal Conditions: A State-of-The-Art Review", *Engineering Structures* 127, pp. 172–188, (2016).
14. Anderberg, Y. and Thelandersson, S., "Stress and Deformation Characteristics of Concrete at High Temperature: 2. Experimental Investigation and Material Behavior Model", *Bull. No. 46, Lund*, (1976).
15. Park, S. H., Manzello, S., L., Bentz, D., P., and Mizukami, T., "Determining Thermal Properties of Gypsum Board at Elevated Temperatures", *Fire and Materials*, (2009), pp. 237-250.
16. Cramer, S.M., Friday, O.M., White, R.H., and Sriprutkiat, G., "Mechanical Properties of Gypsum Board at Elevated Temperatures", *Fire and Materials* (2003) 33–42.
17. Lie, T. T., and Kodur, V. K. R., "Thermal Properties of Fibre Reinforced Concrete at Elevated Temperatures", *National Research Council Canada, Institute for Research in Construction*, 04-01, (1995).
18. Masoud, A.Z., "Structural and Thermal Behaviour of Insulated FRP Strengthened Reinforced Concrete Beams and Slabs in Fire", PhD Thesis, Dept. of Civil Engineering Queen's Univ., Kingston, Ont., Canada, (2013).
19. Lee, J.Y., Oh, Y.J., Park, J., S. and Mansour, M.Y., "Behavior of Concrete Columns Confined with Both Spiral and Fiber Composites", 13th World Conference on Earthquake Engineering, No. 3051, (2004).
20. Hawileh, R., A., Naser, M., Zaidan, W., and Rasheed, H. A., "Modeling of Insulated CFRP Strengthened Reinforced Concrete T-beam Exposed to Fire", *Engineering Structures*, 31( 12) (2009), pp. 3072–3079.